TISSUE ENGINEERING: Part C
Volume 25, Number 12, 2019

DOI: 10.1089/ten.tec.2019.0205

termis
Tissue Engineering
& Regenerative Medicine
International Society

METHODS ARTICLE

Quantifying Vascular Changes Surrounding Bone Regeneration in a Porcine Mandibular Defect Using Computed Tomography

Patricia Carlisle, PhD,[1,2] Jeffrey Marrs, DDS,[1,3] Laura Gaviria, PhD,[4] David T. Silliman, BA,[1] John F. Decker, DDS,[1] Pamela Brown Baer, MEd, DDS,[1,5] and Teja Guda, PhD[4]

Angiogenesis is a critical process essential for optimal bone healing. Several *in vitro* and *in vivo* systems have been previously used to elucidate some of the mechanisms involved in the process of angiogenesis, and at the same time, to test potential therapeutic agents and bioactive factors that play important roles in neovascularization. Computed tomography (CT) is a noninvasive imaging technique that has recently allowed investigators to obtain a diverse range of high-resolution, three-dimensional characterization of structures, such as bone formation within bony defects. Unfortunately, to date, angiogenesis evaluation relies primarily on histology, or *ex vivo* imaging and few studies have utilized CT to qualitatively and quantitatively study the vascular response during bone repair. In the current study a clinical CT-based technique was used to evaluate the effects of rhBMP-2 eluting graft treatment on soft tissue vascular architecture surrounding a large segmental bone defect model in the minipig mandible. The objective of this study was to demonstrate the efficacy of contrast-enhanced, clinical 64-slice CT technology in extracting quantitative metrics of vascular architecture over a 12-week period. The results of this study show that the presence of rhBMP-2 had a positive effect on vessel volume from 4 to 12 weeks, which was explained by a concurrent increase in vessel number, which was also significantly higher at 4 weeks for the rhBMP-2 treatment. More importantly, analysis of vessel architecture showed no changes throughout the duration of the study, indicating therapeutic safety. This study validates CT analysis as a relevant imaging method for quantitative and qualitative analysis of morphological characteristics of vascular tissue around a bone healing site. Also important, the study shows that CT technology can be used in large animal models and potentially be translated into clinical models for the development of improved methods to evaluate tissue healing and vascular adaptation processes over the course of therapy. This methodology has demonstrated sensitivity to tracking spatial and temporal changes in vascularization and has the potential to be applied to studying changes in other high-contrast tissues as well.

Keywords: CT, bone regeneration, vascular morphology, mandible, pig

Impact Statement

Tissue engineering solutions depend on the surrounding tissue response to support regeneration. The inflammatory environment and surrounding vascular supply are critical to determining if therapies will survive, engraftment occurs, and native physiology is restored. This study for the first time evaluates the blood vessel network changes in surrounding soft tissue to a bone defect site in a large animal model, using clinically available computed tomography tools and model changes in vessel number, size, and architecture. While this study focuses on rhBMP2 delivery impacting surrounding vasculature, this validated method can be extended to studying the vascular network changes in other tissues as well.

[1]Dental Trauma and Research Detachment, United States Army Institute of Surgical Research, Fort Sam Houston, San Antonio, Texas.
[2]Prytime Medical Devices, Inc., Boerne, Texas.
[3]School of Dentistry, University of Texas Health Science Center at San Antonio, San Antonio, Texas.
[4]Department of Biomedical Engineering, University of Texas at San Antonio, Texas.
[5]Clinical Operations and New Product Commercialization, GenCure, San Antonio, Texas.
The work was performed primarily at the United States Army Institute of Surgical Research, Fort Sam Houston and at The University of Texas at San Antonio.

Introduction

Bone regeneration is a pressing clinical issue due to an increased clinical presentation of bone loss in traumatic injuries and cancerous resections.[1–3] Disfiguring craniomaxillofacial (CMF) injuries in particular, can result from congenital anomalies of the facial skeleton, oral malignancies such as cancer and infection, or from traumatic injuries.[4–6] Moreover, recent epidemiological studies conducted to evaluate theaters of war in Iraq and Afghanistan have demonstrated an increased frequency of CMF battlefield injuries that approaches 30% of total injuries.[7–10]

The nature of battlefield trauma specifically, has changed since torso and body armor technologies have evolved in the past decade to improve survival. However, evidence has shown that the CMF region is not well protected and is thus left vulnerable to explosive devices and ballistic trauma on the battlefield.[8,9,11] Most CMF battlefield injuries are predominately penetrating soft tissue injuries (58%) characterized by a combination of complex lacerations, tissue avulsions, nerve and vessel injuries, burns, and fractures (27%). Of these, 78% are open fractures and 36% are mandibular fractures.[7–10,12] The complexity of injuries includes extensive damage to surrounding tissues and a lack of sufficient soft tissue coverage in many cases. These issues, especially the lack of functional vasculature, make the wound environment unsuitable to support proper bone healing. Moreover, the low rate of successful outcomes in CMF injuries and the fact that they are rarely seen in civilian trauma makes the situation more challenging to military maxillofacial surgeons.[7,8,10,12,13]

Bone tissue is typically characterized by continuous remodeling, which occurs for the maintenance of overall bone size, shape, and structural integrity.[14] The metabolic and survival activities during bone remodeling are tightly regulated by a multitude of local and systemic factors. These factors control the cellular activities and depend on adequate supply of oxygen, nutrients, hormones, cytokines, and precursor cells from vasculature. Therefore, during injury where normal blood supply is disrupted, inadequate or inappropriate bone vascularity results in fibrous tissue formation and delayed or nonunions.[12,13,15] This is especially important in the case of CMF injuries given the necessity to maintain not just facial esthetics, but also to regenerate bone in the appropriate locations and of sufficient quality to support suitable implants for functional restoration.[10,16] Thus, the regeneration of bone in CMF models needs to be assessed in a holistic manner to include the formation of bone as well as the maintenance of surrounding tissue and vasculature for continued patency of restoration.

Growth factors are important for successful bone regeneration. Specifically, recombinant human bone morphogenetic proteins (rhBMPs), such as rhBMP-2 play essential roles in skeletal embryogenesis, cartilage development, and bone formation. These molecules regulate proliferation, migration, and differentiation of osteoprogenitor and endothelial cells, which are important in the fracture healing process.[14,17,18] The effectiveness of rhBMP-2 has been demonstrated to be significantly improved based on the design of the carrier and the growth factor release system in both extremity segmental bone healing[19] and craniofacial models.[20] However, especially as novel therapeutics progress down the translational pipeline, it is crucial that concerns such as potential inflammation, heterotopic bone growth, and high vascularization[21–23] be studied in large preclinical models to ensure that safe therapeutic windows for growth factors are achieved.

Novel therapeutics include a newer generation of bone graft materials that are often a combination of biomaterial scaffolds to provide suitable substrates, biochemical growth factors to induce tissue-specific differentiation and development, and even suitable biologics such as stem cells to accelerate tissue regeneration.[24–26] In such a complex milieu, the use of preclinical animal models has become the norm for the evaluation of therapeutic safety and efficacy before further approval for translation into clinical applications can be sought. For these reasons, it is crucial to have thorough characterization of the regenerating tissue at all stages of preclinical animal models.

In the current study, we evaluate the effects on surrounding soft tissue vascular architecture in a large segmental bone defect model in the minipig mandible, where one group was left untreated and one group was treated with an rhBMP-2 therapeutic. All minipigs were anesthetized and injected with vascular contrast at five different time points (baseline, 8 weeks after alveolar resection [presegmental], and at three postoperational time points: 4, 8, and 12 weeks after segmental defect creation). Mandibular vascular supply in the minipigs was confirmed and the vasculature was quantified. The objective of this study is to demonstrate the efficacy of contrast-enhanced clinical 64-slice computed tomography (CT) technology to extract quantitative metrics of vascular architecture over time in the same animal, which allows the assessment of therapeutic safety in large animal models and is directly translatable as benchmarking for future clinical use.

Materials and Methods

Experimental design

To evaluate osteogenesis and therapeutic safety in a segmental mandibular bone defect, we created a critical-sized defect (20 cm) in the mandible of dentally mature, female Sinclair minipigs ($n = 12$) (Sinclair BioResources, Columbia, MO). With the animals anesthetized, a two-stage surgical approach was used for this study. First, premolar extraction and alveoplasty was performed on all 12 pigs, followed by an 8-week healing time period. Subsequently, a 20 mm continuity defect was introduced in the right side mandible of each pig. Half of the cohort ($n = 6$) received bone regenerative treatment (polyurethane [PUR]+rhBMP-2, described in detail below) and the remaining animals ($n = 6$) were left untreated. The pigs were allowed to heal for an additional 12 weeks. Multiple parameters were measured to evaluate the impact on vascularity in the surrounding tissues over the course of the study, including vascular network quantification itself (through 64-slice clinical CT scan), and quantifying the local vascular endothelial growth factor (VEGF) secretion profile. The 64-slice CT scans were acquired at baseline (−8 weeks), presegmental defect (0 weeks), and at 4-, 8-, and 12 weeks postsegmental defect, as illustrated in Figure 1. Biological samples used to assess the growth factor profile were collected from the segmental defect surgical site effluent immediately after surgery, and 15 min, 30 min, 1 h, 2 h, 4 h, 8 h, 24 h, and 48 h postsegmental defect creation.

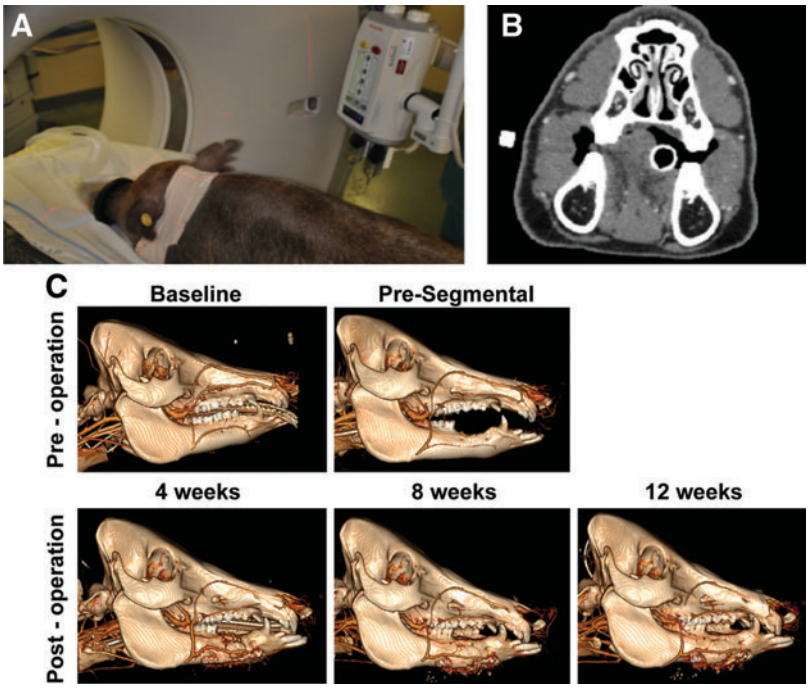

FIG. 1. Minipig vascular evaluation. **(A)** All minipigs in the study were anesthetized and injected with contrast at five different time-points to acquire **(B)** a CT image stack with vessels showing contrast against surrounding soft-tissue. **(C)** Mandibular vascular supply in pigs was confirmed and the vasculature was quantified and analyzed at baseline, 8 weeks after alveolar resection (presegmental) and at three postoperational time points: 4, 8, and 12 weeks after segmental defect creation. CT, computed tomography. Color images are available online.

Animal surgery

This study was conducted in compliance with the Animal Welfare Act, implementing Animal Welfare Regulations, and the principles of the Guide for the Care and Use of Laboratory Animals. To evaluate osteogenesis in a critical-sized mandibular defect model, dentally mature, female Sinclair minipigs (>1 year in age) were used. The pigs underwent two separate surgical procedures. Before both surgical procedures, all animals received anesthetic induction with Telazol (4.4 mg/kg intramuscular) followed by isoflurane (1.5–4%) delivered in 100% oxygen. Following induction, prophylactic antibiotics (Ceftiofur, 5 mg/kg) and prophylactic analgesia were administered. The first procedure was tooth extraction and alveoplasty, and the pigs were placed on their left side and their right side was prepped for surgery. Gingival intrasulcular incisions were made and gingival full-thickness flaps were elevated to aid extractions. Using a surgical handpiece with a side-cutting bur (Micro-Aire, Charlottesville, VA), the three premolars were sectioned and elevated. Alveoplasty was performed to smooth the remaining bone to the root tip using the same side-cutting carbide burr and an oval-cutting carbide burr. The oral mucosa was sutured and the pigs were allowed to heal for 8 weeks before initiation of the second surgical procedure. This 8-week time period was sufficient for full closure and healing of the mucosal tissue.

To initiate the mandibular segmental defect surgery,[27] the pigs were anesthetized and prepped for aseptic surgery and an incision was made along the line of the inferior border of the right mandible. The soft tissue was reflected to expose the mandible and the periosteum was removed from the mandible in the area directly below the tooth extraction location. A titanium stabilizing plate (Synthes, West Chester, PA) was prepositioned with screws and then removed before creation of the segmental bone defect in the mandible; this technique serves to minimize complications with occlusion and anatomical positioning. To introduce the segmental defect, a 2 cm segment was removed using a surgical handpiece with a reciprocating saw (MicroAire). Care was taken to preserve the nerve bundle. Once the bone segment was removed, the titanium reconstruction plate was reaffixed to the mandible using locking and bicortical titanium screws. Half the pigs ($n=6$) received bone regenerative PUR scaffold+rhBMP-2, whereas the second half ($n=6$) remained untreated. Titanium screws were also placed through plate into the scaffold to secure the treatment in place. A Jackson-Pratt drain was placed in the surgical site and the soft tissues were approximated and sutured closed in layers. Biological samples and 64-slice CT scans were collected over the healing time course (as described above) to assess the osteogenic process. All animals were humanely euthanized at 12 weeks postdefect creation (20 weeks from the initial start of the study) using intravenous (IV) injection after anesthesia induction. The United States Army Institute of Surgical Research Institutional Animal Care and Use Committee (IACUC) approved the associated protocol no. A-13-024.

PUR-rhBMP-2 custom graft synthesis

Half of the study subjects ($n=6$) received a PUR-hydroxyapatite β-tricalcium phosphate scaffold impregnated with rhBMP-2. The graft was created as previously reported.[27] Briefly, Lysine-triisocyanate prepolymer (LTI-PEG, 21.7% -NCO group) was purchased from Ricerca Biosciences LLC (Painesville, OH). Glycerol, stannous octoate, and ε-caprolactone were purchased from Sigma-Aldrich (St. Louis, MO). Glycolide and DL-lactide were supplied by Polysciences (Warrington, PA). Triethylene diamine (TEDA) and dipropylene glycol (DPG) were purchased from Sigma-Aldrich and mixed to obtain a 10% (w/w) solution of TEDA in dry DPG. MASTERGRAFT® mini granules (MG) were

obtained from Medtronic, Inc. (Minneapolis, MN). The polyester triol was synthesized as previously described.[28,29] Briefly, glycerol starter was mixed with ε-caprolactone, glycolide, and DL-lactide monomers under argon at 140°C for 40 h. Afterward, the polyester triol was cooled, washed with hexane, and dried under vacuum at 80°C. The backbone of the polyester consisted of 70% ε-caprolactone, 20% glycolide, and 10% DL-lactide, produced at a molecular weight of 450 g/mol.

MG particles were used as received. The rhBMP-2 powder was reconstituted in sterile water, aliquoted into desired doses, and lyophilized before use. The components of the grafts were mixed in a two-step method. In the first step, the polyester triol, MG particles (45 wt%), and TEDA (1.1 pphp) were added to a 10-mL cup and mixed by hand for 30 s. The LTI-PEG and lyophilized rhBMP-2 (100 μg/mL defect) were added to the cup and mixed by hand for 60 s. The index (ratio of isocyanate:hydroxide equivalents × 100) was 115. The reactive mixture was combined with 3 pphp of deionized water, loaded into a straight bore syringe, and injected into a custom scaffold mold to mimic the surgery site. The water drives the foaming reaction of the PUR and the final scaffold reaches a porosity of ∼50%, which has been described previously for these grafts.[30,31] These samples were allowed to cure for 24 h, at 4°C, before removing the composite graft. Any excess graft that overfoamed the mold was shaved off, leaving a porous, implantable biocomposite that would conform to the shape of the defect (Fig. 1D). The final scaffold was weighed to determine the final dose of rhBMP-2 delivered to the animal. The mean delivery dose was calculated to be 0.43 mg/mL rhBMP-2.

64-slice CT

The 64-slice CT (Aquilion 64 Multislice Helical CT Scanner; Toshiba American Medical, Tustin, CA) scans were acquired at baseline (−8 weeks), post-tooth extraction but pre-segmental defect (0 weeks), and at 4-, 8-, and 12 weeks postsegmental defect (Fig. 1). Each scan was performed with Isovue radiopaque contrast media (100 mL through IV catheter) to visualize the vascularization of the bone defect area. The 64-slice CT scan images were acquired at an effective pixel size of 500 μm. Digital Imaging and Communications in Medicine images generated from the scans were converted to bitmap format using trilinear interpolation by a factor of 5 (ImageJ 1.47v; National Institutes of Health) so that the final resolution was 100 μm. DataViewer (Bruker Skyscan, Kontich, Belgium) was used to realign the mandibles along the physiological axes and dentition landmarks were used to ensure that the different time points were all aligned in an identical fashion. The image stack was then imported into CTAn software v1.11 (Bruker Skyscan) and a region of interest (ROI) was created. The ROI was defined posteriorly just before the coronoid process of the mandible and anteriorly by the anterior of the mandibular canine. Manual ROI selection involved the exclusion of the mandibular bone and metallic fixators, which were significantly brighter than the soft tissue in the images (Supplementary Fig. S1). CTAn was then used to perform an initial analysis to acquire a density distribution histogram for each hemimandibular ROI. These initial histograms were compiled for all datasets and then thresholded globally using the Otsu algorithm.[32] The threshold range that identified the contrast-enhanced vasculature corresponded to 30–82 on Grayscale, which is equivalent to 145–573 hounsfield unit (HU). This outcome was utilized to standardize the thresholding for all datasets to differentiate vasculature from surrounding musculoskeletal tissue.[33] Measurements were made using CTAn software to assess vessel volume, vessel architecture (shape, diameter, and vascular tree organization), and vessel number across the three-dimensional ROI. Data for each pig were normalized to measurements from their nonsurgical contralateral hemimandible and reported relative to their presurgical baseline measurements.

Biological sample collection and protein detection assays

To measure the presence of VEGF in the early wound healing environment, we collected drainage samples from the Jackson-Pratt drain, which had been placed in the surgical site immediately after introduction of the segmental mandibular bone defect. We collected drain fluid samples at 0-, 15-, and 30 min and 1-, 2-, 4-, 8-, 24-, and 48 h postsurgery. The drain was no longer productive after the48-h time point. The drain fluid samples were centrifuged at 1300 × *g* for 15 min at 4°C to remove cells and debris. Supernatant was stored at −80°C. Quantification of VEGF protein in the serum, saliva, and drain fluid samples was performed using the Human Luminex bead-based multiplex assay (R&D Systems, Minneapolis, MN). Each sample was run in duplicate on the Luminex platform as per the manufacturer's instructions. The fluorescence readings were taken using the Bio-Plex200 System (Bio-Rad, Hercules, CA).

Statistical analysis

All data are reported as mean ± standard error of the mean. Two-way repetitive measures analysis of variance (ANOVA) was used for statistical analysis of protein content data from saliva, serum, and drain fluid. If the treatment/time interaction effect was significant, then *post hoc* pairwise comparisons were performed using Bonferroni adjustment. If the treatment/time interaction effect was not significant, then area under the curve analysis was performed. Statistical analysis of 64-slice CT data was performed using two-way ANOVA (across time and treatment) and *post hoc* testing of significance was performed using Tukey's test. The statistical analysis on the protein data for the oral mouth wash was performed after the raw data were normalized to the total protein concentration for each wash sample and log transformed. The drain fluid and serum raw data were log transformed before statistical analysis.

Results

Animal model observations

Contrast enhancement using the Isovue radiopaque contrast media was observed to be effective in highlighting vasculature in comparison to the surrounding soft tissue. The 3D rendering software extracted the facial and mental arteries and their vascular branches around the mandible and was able to qualitatively indicate changes over time (Fig. 1). Even in the swollen callus formed around the rhBMP-2-based therapy, the vessels were clearly identifiable. The extraction methodology employed using selective soft tissue regions of interest, resulted in the separation of the vascular network from the coronoid process of the mandible to the

anterior of the mandibular canine providing comparable datasets for quantification. Employing identical anatomical landmarks and analyzing the contralateral hemimandible vasculature as a controlled comparison enabled tracking the architecture of vessel networks over time in a consistent fashion (Fig. 2).

VEGF expression in drain fluid

Surgical drain fluid effluent was analyzed for the production of VEGF over the first 48 h following segmental defect creation surgery. VEGF protein expression remained low during the first 2 h postsurgery in both the untreated (31.82 ± 9.50 pg/mL) and the rhBMP-2-treated groups (31.34 ± 6.42 pg/mL), but increased consistently in both the untreated (6.07 ± 4.92 pg/mL·h) and the rhBMP-2-treated groups (8.17 ± 2.63 pg/mL·h) until the assessment at 48 h postsurgery. The expression of VEGF was significantly greater ($p < 0.05$) in the rhBMP-2 therapy group (319.22 ± 33.61 pg/mL) compared with the untreated group (229.95 ± 43.33 pg/mL) only 24 h after surgery (Fig. 4). The statistical analysis of the VEGF drain data was neither normally distributed (Shapiro–Wilk test, $p < 0.05$) nor were the variances in groups equal (Brown–Forsythe test, $p < 0.05$), resulting data being assessed, the general linear model followed by pairwise comparisons using Tukey's *post hoc* test. For both groups, the 24- and 48-h VEGF production levels were greater than those observed over any of the time points during the first 4 h of collection (Fig. 3).

No VEGF was detected in serum within the sensitivity range of the kit at any time point during the study. Saliva wash samples were normalized to presurgery levels for each animal to reduce intragroup variations, and showed detectable VEGF protein levels with trends that matched the drain fluid effluent over the first 48 h after either surgery (Supplementary Fig. S2A, B). Furthermore, stabilization of VEGF levels was observed across the entire duration of the animal model (Supplementary Fig. S2C), with no difference observed between the rhBMP-2-treated and untreated groups at individual time points. Surgical drain fluid effluent over the first 48 h following segmental defect creation surgery was also analyzed for the production of angiopoietin 2 (ANG2), basic fibroblast growth factor (FGF2), placental growth factor (PLGF), and BMP9, all of which have been variously implicated in the promotion and stabilization of capillary and vessel networks. ANG2 and FGF2 were present at elevated levels over the first

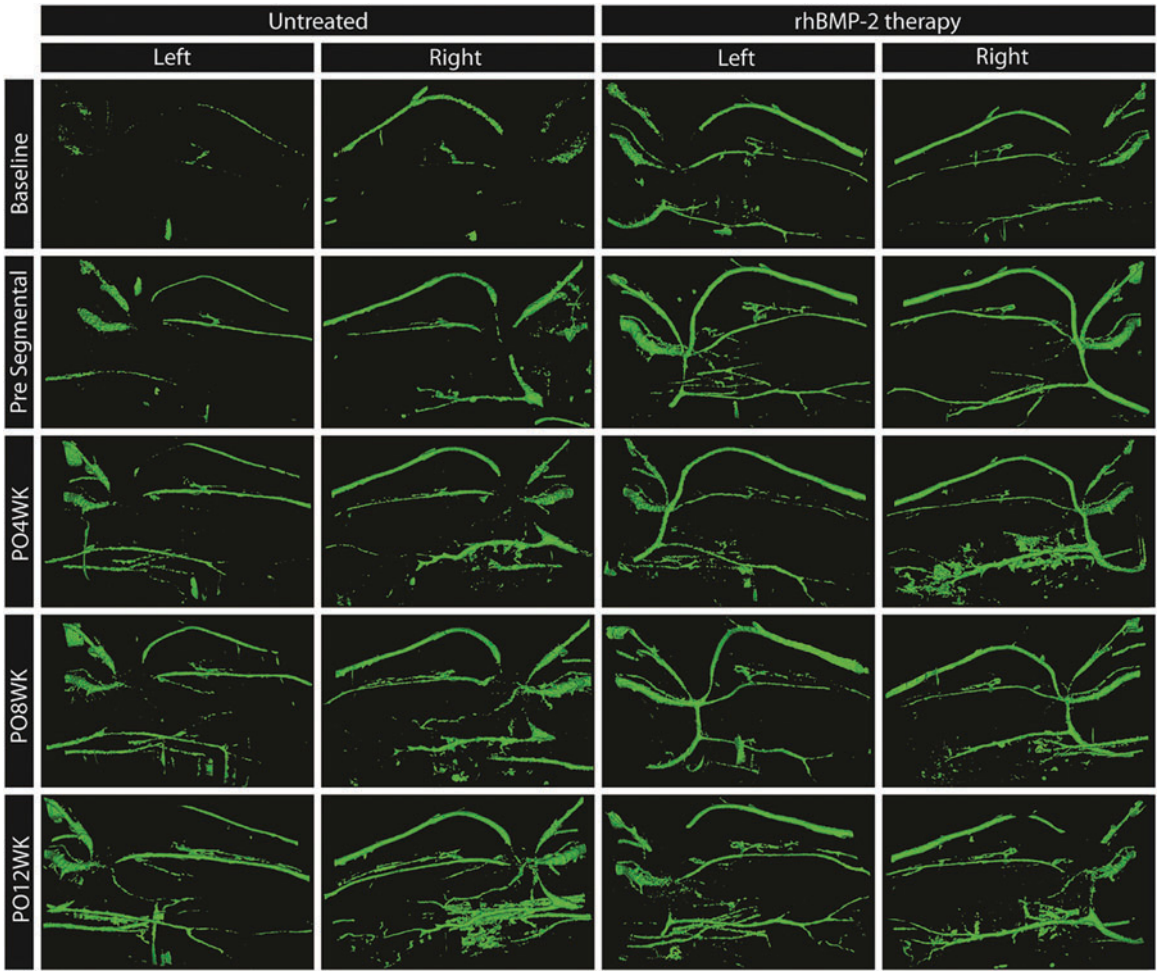

FIG. 2. Extracted CT images of mandibular vasculature. The contrast-enhanced vasculature is reconstructed in 3D and a lingual view is captured for representative minipigs from the untreated defect and rhBMP-2 therapy groups at baseline, presegmental, and 4, 8, and 12 weeks postsurgery. Color images are available online.

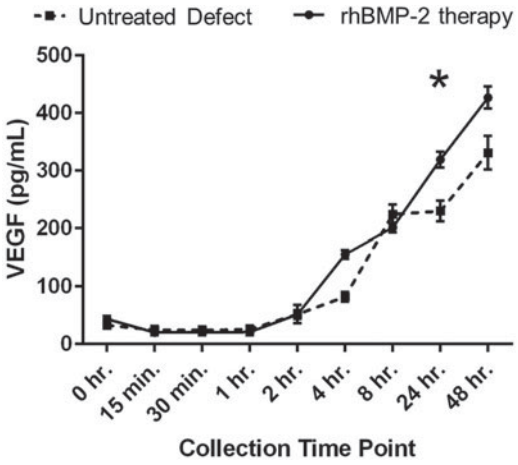

FIG. 3. VEGF expression postsurgery. Surgical drain fluid effluent was analyzed for the production of VEGF over the first 48 h following segmental defect creation surgery. While VEGF protein expression increased after the first 2 h postsurgery in both the untreated and the rhBMP-2-treated groups, the expression was significantly greater in the rhBMP-2 therapy group only 24 h after surgery (*$p < 0.05$). VEGF, vascular endothelial growth factor.

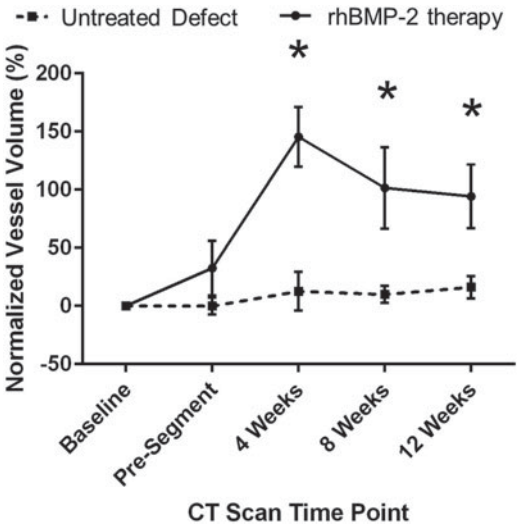

FIG. 4. Increase in vessel volume with rhBMP-2 treatment. At 4, 8, and 12 weeks after segmental defect restoration, the rhBMP-2-treated group had a significantly greater normalized vessel volume compared with the no-treatment group (*$p < 0.05$). No differences were observed before segmental defect creation.

2 h and dropped to significantly lower levels by 8 h in both treatment groups (Supplementary Fig. S3A, B; $p < 0.0001$). There were no significant differences between treatment groups at any time points for either ANG2 or FGF2. No significant changes were seen in PLGF at any time within either treatment group and no BMP9 was detected for any sample (Supplementary Fig. S3C, D).

Quantification of vessel architecture using contrast-enhanced CT

Vessel volume was significantly higher at 4 ($p < 0.001$), 8 ($p = 0.014$) and 12 weeks ($p = 0.033$) after segmental defect restoration in the rhBMP-2-treated group ($204.41 \pm 8.34\ mm^3$ at 4 weeks, $164.74 \pm 14.26\ mm^3$ at 8 weeks, $165.21 \pm 20.42\ mm^3$ at 12 weeks), compared with the untreated group ($112.59 \pm 10.56\ mm^3$ at 4 weeks, $116.26 \pm 4.13\ mm^3$ at 8 weeks, $141.36 \pm 25.26\ mm^3$ at 12 weeks). The vessel volume data normalized to the contralateral hemimandible vessel volume to adjust for variance between animals is shown in Figure 4.

The vessel number was found to be significantly higher 4 weeks after segmental defect restoration in the rhBMP-2-treated group ($163.1 \pm 17.8\ mm^3$) compared with the untreated group ($123.4 \pm 21.3\ mm^3$, $p = 0.011$). This trend continued over the healing time period ($p = 0.251$ after 8 weeks and $p = 0.058$ after 12 weeks), suggesting that angiogenesis was enhanced in the rhBMP-2-treated group. The quantification of the vessel number between treatments over time is shown in Figure 5. No significant changes were observed over time or between treatments in vessel architecture across vessel surface to volume ratio (aspect ratio), mean vessel size (diameter), or vessel pattern factor (branching morphology), as seen in Figure 6.

Discussion

The role of concomitant angiogenesis is essential for physiological bone remodeling and sustainable regeneration.[12,13,15,34–36] VEGF has been extensively implicated as one of the key mediators in this process[14,15,37,38] for its ability to act as a potent mitogen as well as to induce a strong angiogenic response. The role of VEGF in the vascularization (e.g., the expansion of capillary beds within developing bones) of bone tissue and in bone homeostasis have also been well characterized.[14,15,37–41] The recapitulation of these processes is also essential for the maintenance of appropriate callus architecture and subsequent mineralization in response to bone injury.[38,42] Recently, it has been proposed that the synergistic effect of VEGF and

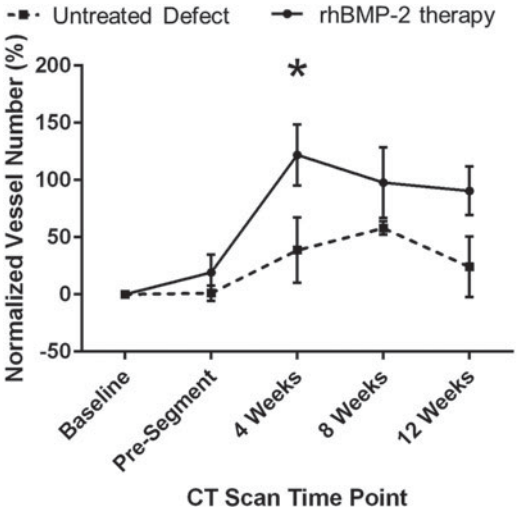

FIG. 5. Increase in vessel volume due to increase in vessel number. The changes in normalized vessel number were similar to the trends seen in vessel volume. The normalized vessel number in the rhBMP-2-treated group was significantly greater at 4 weeks after segmental defect restoration compared with the no-treatment group (*$p < 0.05$).

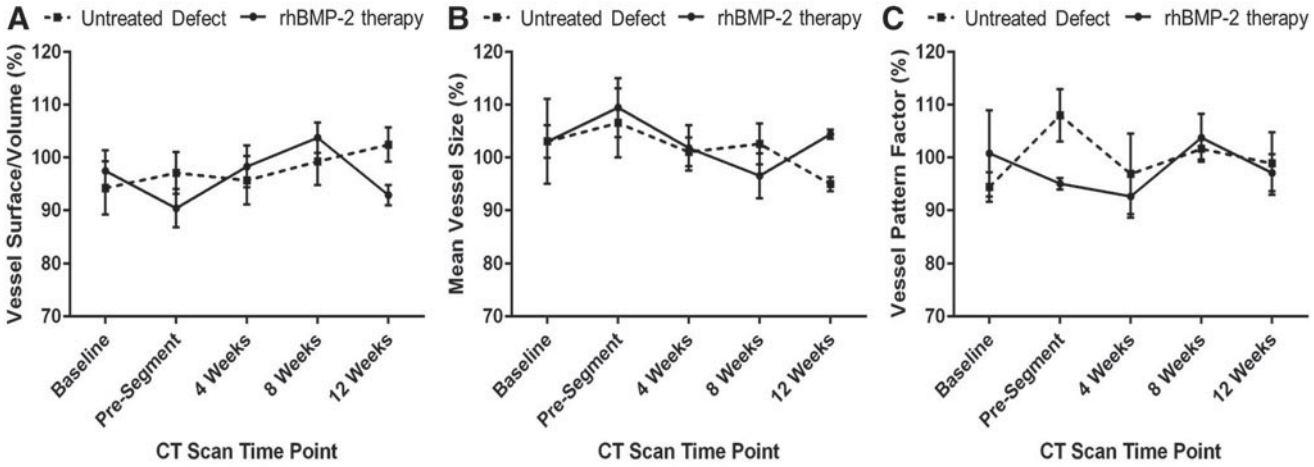

FIG. 6. No changes in vessel architecture. No changes in vessel architectural parameters, including **(A)** vessel surface to volume ratio, **(B)** mean vessel size, and **(C)** vessel pattern factor were observed between groups or at different time points, indicating that native vessel physiology and vascular tree architecture was maintained.

rhBMP-2 can mimic the natural bone development process and result in more effective bone regeneration in critical-sized bone defects or compromised bones that have insufficient vascularization.[37,43–46]

In this study, we evaluated if treatment with rhBMP-2 in a porcine mandible segmental defect site had an effect on VEGF expression *in vivo,* especially in the surrounding soft tissue. It was observed (Fig. 3) that while VEGF protein expression did increase during the postsurgery time points, this change was not dependent on rhBMP-2 at the early time points and only 24 h after surgery, was a significantly greater expression of VEGF observed. Past research by Hussein *et al.* hypothesized that the delivery of rhBMP2 at bone defect sites in the CMF skeleton mediated the further expression of endogenous BMP2 and VEGF from the surrounding soft tissue.[47,48] Our results further corroborate this hypothesis.

Other observations indicated that there was an immediate expression of ANG2 and FGF2 after segmental defect creation and implantation; irrespective of whether the graft contained rhBMP-2. Previous reports indicate that the local delivery of FGF2 even in a single dose resulted in improved bone callus formation and robust angiogenesis,[49] especially in a dose-dependent manner in craniofacial bone defect models.[50] ANG2, while an endogenous antagonist of Tie2 signaling and thus antiangiogenic, has been shown to modulate and stabilize neoangiogenic sprouts and thus lead to vessel maturation,[51] with local delivery of ANG2 showing concurrent callus growth and robust angiogenesis in bone healing models.[52] The early observations of ANG2 and FGF2 in this model from the drain fluid thus indicates a robust prohealing response from the tissue bed postsurgery, with no differences observable between groups indicating this is likely an effect of the surgical procedure rather than the specific graft implanted.

Angiogenesis has been studied using numerous *in vitro* and *in vivo* systems with the purpose of elucidating the mechanisms involved in the process of angiogenesis and testing potential therapeutic agents and bioactive factors that inhibit or promote neovascularization.[53–63] Although other studies have observed vascularization using histology slices, the major limitation of this technique is that observation and quantification are limited to one time point per animal and to a limited number of locations,[21] which may not permit the quantification of vascular network architecture.[64] To evaluate and assess the impact of injury and healing on the vessel network, the structure and function of the new vasculature should be quantifiable; newly formed vessels should be distinguished from preexisting vessels; long-term and noninvasive monitoring should be possible; and the system should be economical, quick, simple, reproducible, and reliable. Therefore, although a wide variety of *in vitro* and *in vivo* assays exist, there is as yet no standardized measure of angiogenesis, quantification is often absent, and the results are not necessarily applicable or easily translatable to the clinical setting.[31,53,65–67]

In the current study we used clinical CT (clinical 64-slice CT) to evaluate the therapeutic effect of rhBMP-2 on surrounding soft tissue vascular architecture in a large segmental bone defect model in the minipig mandible. Contrast enhancement of the vasculature was performed using Isovue radiopaque contrast, which allowed the vessels to be easily distinguished from the surrounding soft tissue. As increased research efforts are focused on the development of prevascularized bone,[68–70] contrast perfusion-based detection of vascularization can also serve as a nondestructive quantification of functional restoration of vascularization deficits. The results of this study showed rhBMP-2-dependent increases in vessel volume for up to 12 weeks postrestorative surgery, and that total vessel volume was greater at all times after segmental defect restoration compared with before segmental defect creation (Fig. 4). Quantification of the vascular network architecture attributed these changes in vessel volume to changes in vessel number (Fig. 5) and not to changes in vessel architecture (Fig. 6A–C); suggesting evidence for physiological angiogenesis as well as vascular adaptation during rhBMP-2-induced bone regeneration and healing.

Historically, characterization of tissue vascularization has only been evaluated using histological sample preparation and staining leading to quantification that is limited to the number of vessels observed in selected fields of view.[71–74] *In vivo* noninvasive techniques that provide a true approximation of the 3D vascular network are required to recapitulate and understand the complex process of vessel formation

under physiological and pathological conditions.[53,65,75,76] Although some techniques are currently being developed in almost all imaging modalities (ultrasound, single-photon emission computed tomography [SPECT], positron emission tomography [PET], magnetic resonance imaging [MRI], CT, etc.),[75,77,78] studies to date have focused predominantly on MRI and radionuclide techniques, such as SPECT and PET imaging.[77] CT on the other hand, has replaced histology and has emerged as a standard platform for the assessment of bone regeneration.[79] With its current use in the field and relative ease of access, it is an ideal, promising technology for overcoming the challenges associated with the evaluation of vascular networks *in vivo*.[80] CT allows the performance of multiple scans over time by noninvasively tracking changes, and therefore, reducing the time and number of animals needed.[28–30,80]

Quantitative analysis of vascularization using micro-CT relies on the observation of the 3D vascular structure without the limitation of sectioning the specimen and yields better resolution in comparison with other techniques (i.e., histology) allowing the investigators to obtain a diverse range of high-resolution, 3-dimensional characterization of structures that calculate vessel numbers from the entire vascular tree.[28–31,33,80] So far, quantification of angiogenesis using micro-CT has been used to evaluate microvascular architecture of different organs (kidney, heart, bone, liver), tumors, and tissue-engineered constructs.[29,31] However, the downside of using the micro-CT modality, is that it is only suitable for small animal models, and not for clinical diagnoses due to equipment size restrictions and radiation exposure doses.[28–30,80]

To the best of our knowledge, while some studies have used micro-CT to qualitatively and quantitatively study the vascular response during bone repair,[31,53] none has utilized clinically accessible 64-slice CT to study vascular networks. A modality such as clinical CT (64 slice or better resolution) is especially necessary for large animal models to truly get an understanding of the changes in the vascular tree at scales that have clinical significance and over scan times and settings that are potentially translatable. A good CMF animal model that could produce data transferable to humans is the minipig due to the functional and anatomical similarities in the mandibular blood supply.[66] Adult dentitions were critical to the current large animal model, since the nature of bone regeneration and potentially surrounding tissue response are very different in immature pigs as compared with fully mature adults (>1 year of age). Since only female pigs in the established Sinclair minipig models are available in this age range, only female pigs were tested in the current model. Gender-specific differences in the response of the local vascularity and the response to rhBMP-2 delivery were not tested in this study. Since angiogenesis is critical to optimal bone healing, developing techniques and better animal models to temporally measure vascularization would significantly enhance our ability to evaluate the success of bone regenerative treatment modalities.

The three metrics used in the current study to evaluate vessel architecture (Fig. 6A: vessel surface to volume ratio, Fig. 6B: mean vessel size, and Fig. 6C: vessel pattern factor) did not show changes through the duration of the study with no statistically significant differences noted either between groups or within one group over time. This means that there were no changes in the vascular architecture, organization, or physiology of the animals during the study (vessel shape, vessel diameter, and vascular tree organization); indicating maintenance of a physiological phenotype as well as therapy safety. Vessel number was greater at all times after segmental defect restoration compared with baseline, and was significantly higher 4 weeks after segmental defect restoration in the rhBMP-2 group compared with the untreated group (Fig. 5). This trend continued over the healing time period and suggests that sustainable angiogenesis was enhanced in the rhBMP-2-treated group.

Although the vasculature is essential for embryonic development, postnatal growth, and bone remodeling,[13–15,81] the morphogenetic events that occur during the formation of new blood vessels are not completely understood.[77,81,82] Previous evidence *in vitro* has demonstrated that there is intercellular communication, codependency, and regulation of cell activities between bone and endothelial cells.[12,14,15,37,38,83] Temporal *in vivo* imaging and quantification of the bone vessel network are essential in understanding the complex process of angiogenesis under physiological and pathological conditions[75]; and at present, there is a need to develop noninvasive and automated imaging strategies to track the *in vivo* spatial distribution and temporal characteristics of angiogenesis to assess the efficacy of angiogenic therapies in preclinical animal models.[31,75]

As shown in this study, one of the advantages of using high-resolution CT is the ability to study the entire vascular tree in terms of its 3D morphometric parameters, allowing quantification for better understanding of the exact nature of vascular adaptation during regeneration. More importantly, this study demonstrates the efficacy of contrast-enhanced clinical 64-slice CT technology to extract quantitative metrics of vascular architecture over time in a large animal model, which also demonstrates its clinical significance and its translation potential for evaluation of bone regenerative treatment modalities.

Conclusions

In the current study, a clinical CT-based technique to quantify vascular changes in surrounding tissue during bone regenerative treatment using contrast enhancement was validated in a large animal preclinical model. We showed that both quantitative and qualitative methods of CT analysis can be used to establish the unique morphological characteristics of the vascular network and changes associated with both empty and scaffold-implanted bone defects. We also found that rhBMP-2 therapy enhances angiogenesis compared with untreated groups, increasing vessel number as well as vessel volume, while demonstrating maintenance of physiological phenotype and therapy safety. Moreover, we demonstrated the efficacy of contrast-enhanced clinical 64-slice CT technology for preclinical and potentially clinical model development to enhance evaluation of the bone healing process and surrounding soft tissue coverage over the course of therapy.

Acknowledgments

The views expressed in this article are those of the authors and do not reflect the official policy or position of the U.S. Army Medical Department, Department of the Army,

DoD, or the U.S. Government. Research was conducted in compliance with the Animal Welfare Act, the implementing Animal Welfare regulations, and the principles of the Guide for the Care and Use of Laboratory Animals, National Research Council. The facility's Institutional Animal Care and Use Committee approved all research conducted in this study. The facility where this research was conducted is fully accredited by Association for Assessment and Accreditation of Laboratory Animal Care (AAALAC).

Disclosure Statement

No competing financial interests exist.

Funding Information

This study was primarily supported by funding from the United States Army Medical Research and Materiel Command and the Department of Defense. TG was also supported by National Science Foundation award #1847103.

Supplementary Material

Supplementary Figure S1
Supplementary Figure S2
Supplementary Figure S3

References

1. Henkel, J., Woodruff, M.A., Epari, D.R., *et al.* Bone regeneration based on tissue engineering conceptions—a 21st century perspective. Bone Res **1,** 216, 2013.
2. Liu, Y., Moller, B., Wiltfang, J., Warnke, P.H., and Terheyden, H. Tissue engineering of a vascularized bone graft of critical size with an osteogenic and angiogenic factor-based *in vivo* bioreactor. Tissue Eng Part A **20,** 3189, 2014.
3. Horner, E.A., Kirkham, J., Wood, D., *et al.* Long bone defect models for tissue engineering applications: criteria for choice. Tissue Eng Part B Rev **16,** 263, 2010.
4. He, X., Dziak, R., Mao, K., *et al.* Integration of a novel injectable nano calcium sulfate/alginate scaffold and BMP2 gene-modified mesenchymal stem cells for bone regeneration. Tissue Eng Part A **19,** 508, 2013.
5. Wolf, D.E., Seetamraju, M., Gurjar, R.S., Kuo, R.S., Fasi, A., and Feinberg, S.E. Non-invasive monitoring of vascularization of grafted engineered human oral mucosa. Proc SPIE **8222,** 2012; DOI: 10.1117/12.909032.
6. Buyukdereli, G., Guney, I.B., Ozerdem, G., and Kesiktas, E. Evaluation of vascularized graft reconstruction of the mandible with Tc-99m MDP bone scintigraphy. Ann Nucl Med **20,** 89, 2006.
7. Hale, R.G., Lew, T., and Wenke, J.C. Craniomaxillofacial battle injuries: injury patterns, conventional treatment limitations and direction of future research. Singapore Dent J **31,** 1, 2010.
8. Lew, T.A., Walker, J.A., Wenke, J.C., Blackbourne, L.H., and Hale, R.G. Characterization of craniomaxillofacial battle injuries sustained by United States service members in the current conflicts of Iraq and Afghanistan. J Oral Maxillofac Surg **68,** 3, 2010.
9. Chan, R.K., Siller-Jackson, A., Verrett, A.J., Wu, J., and Hale, R.G. Ten years of war: a characterization of craniomaxillofacial injuries incurred during operations Enduring Freedom and Iraqi Freedom. J Trauma Acute Care Surg **73,** S453, 2012.
10. Brown Baer, P.R., Wenke, J.C., Thomas, S.J., and Hale, C.R. Investigation of severe craniomaxillofacial battle injuries sustained by U.S. Service members: a case series. Craniomaxillofac Trauma Reconstr **5,** 243, 2012.
11. Madson, A.Q., Tucker, D., Aden, J., Hale, R.G., and Chan, R.K. Non-battle craniomaxillofacial injuries from U.S. military operations. J Craniomaxillofac Surg **41,** 816, 2013.
12. Carano, R.A., and Filvaroff, E.H. Angiogenesis and bone repair. Drug Discov Today **8,** 980, 2003.
13. Cao, L., Wang, J., Hou, J., Xing, W., and Liu, C. Vascularization and bone regeneration in a critical sized defect using 2-N,6-O-sulfated chitosan nanoparticles incorporating BMP-2. Biomaterials **35,** 684, 2014.
14. Chim, S.M., Tickner, J., Chow, S.T., *et al.* Angiogenic factors in bone local environment. Cytokine Growth Factor Rev **24,** 297, 2013.
15. Clarkin, C.E., and Gerstenfeld, L.C. VEGF and bone cell signalling: an essential vessel for communication? Cell Biochem Funct **31,** 1, 2013.
16. Tatara, A.M., Wong, M.E., and Mikos, A.G. *In vivo* bioreactors for mandibular reconstruction. J Dent Res **93,** 1196, 2014.
17. Chenard, K.E., Teven, C.M., He, T.C., and Reid, R.R. Bone morphogenetic proteins in craniofacial surgery: current techniques, clinical experiences, and the future of personalized stem cell therapy. J Biomed Biotechnol **2012,** 601549, 2012.
18. Raida, M., Heymann, A.C., Gunther, C., and Niederwieser, D. Role of bone morphogenetic protein 2 in the crosstalk between endothelial progenitor cells and mesenchymal stem cells. Int J Mol Med **18,** 735, 2006.
19. Brown, K.V., Li, B., Guda, T., Perrien, D.S., Guelcher, S.A., and Wenke, J.C. Improving bone formation in a rat femur segmental defect by controlling bone morphogenetic protein-2 release. Tissue Eng Part A **17,** 1735, 2011.
20. Dumas, J.E., BrownBaer, P.B., Prieto, E.M., *et al.* Injectable reactive biocomposites for bone healing in critical-size rabbit calvarial defects. Biomed Mater (Bristol, Engl) **7,** 024112, 2012.
21. Yudell, R.M., and Block, M.S. Bone gap healing in the dog using recombinant human bone morphogenetic protein-2. J Oral Maxillofac Surg **58,** 761, 2000.
22. Wikesjo, U.M., Qahash, M., Thomson, R.C., *et al.* rhBMP-2 significantly enhances guided bone regeneration. Clin Oral Implants Res **15,** 194, 2004.
23. Haidar, Z.S., Hamdy, R.C., and Tabrizian, M. Delivery of recombinant bone morphogenetic proteins for bone regeneration and repair. Part A: current challenges in BMP delivery. Biotechnol Lett **31,** 1817, 2009.
24. Schroeder, J.E., and Mosheiff, R. Tissue engineering approaches for bone repair: concepts and evidence. Injury **42,** 609, 2011.
25. Giannoudis, P., Psarakis, S., and Kontakis, G. Can we accelerate fracture healing? A critical analysis of the literature. Injury **38 (Suppl. 1),** S81, 2007.
26. Giannoudis, P.V., Einhorn, T.A., Schmidmaier, G., and Marsh, D. The diamond concept—open questions. Injury **39 (Suppl. 2),** S5, 2008.
27. Carlisle, P., Guda, T., Silliman, D.T., *et al.* Localized low-dose rhBMP-2 is effective at promoting bone regeneration in mandibular segmental defects. J Biomed Mater Res Part B Appl Biomater **107,** 1491, 2019.

28. Duvall, C.L., Taylor, W.R., Weiss, D., and Guldberg, R.E. Quantitative microcomputed tomography analysis of collateral vessel development after ischemic injury. Am J Physiol Heart Circ Physiol **287,** H302, 2004.
29. Rai, B., Oest, M.E., Dupont, K.M., Ho, K.H., Teoh, S.H., and Guldberg, R.E. Combination of platelet-rich plasma with polycaprolactone-tricalcium phosphate scaffolds for segmental bone defect repair. J Biomed Mater Res Part A **81,** 888, 2007.
30. Guldberg, R.E., Lin, A.S., Coleman, R., Robertson, G., and Duvall, C. Microcomputed tomography imaging of skeletal development and growth. Birth Defects Res C Embryo Today Rev **72,** 250, 2004.
31. Arkudas, A., Beier, J.P., Pryymachuk, G., *et al.* Automatic quantitative micro-computed tomography evaluation of angiogenesis in an axially vascularized tissue-engineered bone construct. Tissue Eng Part C Methods **16,** 1503, 2010.
32. Otsu, N. A threshold selection method from gray-level histograms. IEEE Trans Syst man Cybern **9,** 62, 1979.
33. Guda, T., Darr, A., Silliman, D.T., *et al.* Methods to analyze bone regenerative response to different rhBMP-2 doses in rabbit craniofacial defects. Tissue Eng Part C Methods **20,** 749, 2014.
34. Roux, B.M., Cheng, M.H., and Brey, E.M. Engineering clinically relevant volumes of vascularized bone. J Cell Mol Med **19,** 903, 2015.
35. Saran, U., Gemini Piperni, S., and Chatterjee, S. Role of angiogenesis in bone repair. Arch Biochem Biophys **561,** 109, 2014.
36. Weigand, A., Beier, J.P., Hess, A., *et al.* Acceleration of vascularized bone tissue-engineered constructs in a large animal model combining intrinsic and extrinsic vascularization. Tissue Eng Part A **21,** 1680, 2015.
37. Keramaris, N.C., Calori, G.M., Nikolaou, V.S., Schemitsch, E.H., and Giannoudis, P.V. Fracture vascularity and bone healing: a systematic review of the role of VEGF. Injury **39 (Suppl. 2),** S45, 2008.
38. Yang, Y.Q., Tan, Y.Y., Wong, R., Wenden, A., Zhang, L.K., and Rabie, A.B. The role of vascular endothelial growth factor in ossification. Int J Oral Sci **4,** 64, 2012.
39. Hu, K., and Olsen, B.R. Osteoblast-derived VEGF regulates osteoblast differentiation and bone formation during bone repair. J Clin Invest **126,** 509, 2016.
40. Hu, K., and Olsen, B.R. Vascular endothelial growth factor control mechanisms in skeletal growth and repair. Dev Dyn **246,** 227, 2017.
41. Zhang, W., Zhu, C., Wu, Y., *et al.* VEGF and BMP-2 promote bone regeneration by facilitating bone marrow stem cell homing and differentiation. Eur Cells Mater **27,** 1, 2014.
42. Sivakumar, B., Harry, L.E., and Paleolog, E.M. Modulating angiogenesis: more vs less. JAMA **292,** 972, 2004.
43. Samee, M., Kasugai, S., Kondo, H., Ohya, K., Shimokawa, H., and Kuroda, S. Bone morphogenetic protein-2 (BMP-2) and vascular endothelial growth factor (VEGF) transfection to human periosteal cells enhances osteoblast differentiation and bone formation. J Pharmacol Sci **108,** 18, 2008.
44. Xiao, C., Zhou, H., Liu, G., *et al.* Bone marrow stromal cells with a combined expression of BMP-2 and VEGF-165 enhanced bone regeneration. Biomed Mater (Bristol, Engl) **6,** 015013, 2011.
45. An, G., Zhang, W.B., Ma, D.K., *et al.* Influence of VEGF/BMP-2 on the proliferation and osteogenetic differentiation of rat bone mesenchymal stem cells on PLGA/gelatin composite scaffold. Eur Rev Med Pharmacol Sci **21,** 2316, 2017.
46. Li, B., Wang, H., Qiu, G., Su, X., and Wu, Z. Synergistic effects of vascular endothelial growth factor on bone morphogenetic proteins induced bone formation *in vivo*: influencing factors and future research directions. BioMed Res Int **2016,** 2869572, 2016.
47. Hussein, K.A., Zakhary, I.E., Elawady, A.R., *et al.* Difference in soft tissue response between immediate and delayed delivery suggests a new mechanism for recombinant human bone morphogenetic protein 2 action in large segmental bone defects. Tissue Eng Part A **18,** 665, 2012.
48. Howie, R.N., Borke, J.L., Kurago, Z., *et al.* A model for osteonecrosis of the jaw with zoledronate treatment following repeated major trauma. PLoS One **10,** e0132520, 2015.
49. Hankenson, K.D., Dishowitz, M., Gray, C., and Schenker, M. Angiogenesis in bone regeneration. Injury **42,** 556, 2011.
50. Kigami, R., Sato, S., Tsuchiya, N., Yoshimakai, T., Arai, Y., and Ito, K. FGF-2 angiogenesis in bone regeneration within critical-sized bone defects in rat calvaria. Implant Dent **22,** 422, 2013.
51. Wu, Y., Chen, L., Scott, P.G., and Tredget, E.E. Mesenchymal stem cells enhance wound healing through differentiation and angiogenesis. Stem Cells **25,** 2648, 2007.
52. Yin, J., Gong, G., Sun, C., *et al.* Angiopoietin 2 promotes angiogenesis in tissue-engineered bone and improves repair of bone defects by inducing autophagy. Biomed Pharmacother **105,** 932, 2018.
53. Young, S., Kretlow, J.D., Nguyen, C., *et al.* Microcomputed tomography characterization of neovascularization in bone tissue engineering applications. Tissue Eng Part B Rev **14,** 295, 2008.
54. Mahmoud, A.M., Sandoval, C., Teng, B., *et al.* High-resolution vascular tissue characterization in mice using 55MHz ultrasound hybrid imaging. Ultrasonics **53,** 727, 2013.
55. Nebuloni, L., Kuhn, G.A., Vogel, J., and Muller, R. A novel *in vivo* vascular imaging approach for hierarchical quantification of vasculature using contrast enhanced microcomputed tomography. PLoS One **9,** e86562, 2014.
56. Santoni, B.G., Ehrhart, N., Betancourt-Benitez, R., Beck, C.A., and Schwarz, E.M. Quantifying massive allograft healing of the canine femur *in vivo* and *ex vivo*: a pilot study. Clin Orthop Relat Res **470,** 2478, 2012.
57. Seo, Y., Hashimoto, T., Nuki, Y., and Hasegawa, B.H. *In vivo* microCT imaging of rodent cerebral vasculature. Phys Med Biol **53,** N99, 2008.
58. Upputuri, P.K., Sivasubramanian, K., Mark, C.S., and Pramanik, M. Recent developments in vascular imaging techniques in tissue engineering and regenerative medicine. BioMed Res Int **2015,** 783983, 2015.
59. Wang, H., Zheng, L.F., Feng, Y., *et al.* A comparison of 3D-CTA and 4D-CE-MRA for the dynamic monitoring of angiogenesis in a rabbit VX2 tumor. Eur J Radiol **81,** 104, 2012.
60. van den Wijngaard, J.P., Schwarz, J.C., van Horssen, P., *et al.* 3D imaging of vascular networks for biophysical modeling of perfusion distribution within the heart. J Biomech **46,** 229, 2013.
61. Zagorchev, L., Oses, P., Zhuang, Z.W., *et al.* Micro computed tomography for vascular exploration. J Angiogenes Res **2,** 7, 2010.

62. Zhao, F., Liu, J., Qu, X., *et al. In vivo* quantitative evaluation of vascular parameters for angiogenesis based on sparse principal component analysis and aggregated boosted trees. Phys Med Biol **59,** 7777, 2014.
63. Zhao, F., Liang, J., Chen, X., *et al.* Quantitative analysis of vascular parameters for micro-CT imaging of vascular networks with multi-resolution. Med Biol Eng Comput **54,** 511, 2016.
64. Dellian, M., Witwer, B.P., Salehi, H.A., Yuan, F., and Jain, R.K. Quantitation and physiological characterization of angiogenic vessels in mice: effect of basic fibroblast growth factor, vascular endothelial growth factor/vascular permeability factor, and host microenvironment. Am J Pathol **149,** 59, 1996.
65. Irvin, M.W., Zijlstra, A., Wikswo, J.P., and Pozzi, A. Techniques and assays for the study of angiogenesis. Exp Biol Med (Maywood, NJ) **239,** 1476, 2014.
66. Saka, B., Wree, A., Henkel, K.O., Anders, L., and Gundlach, K.K. Blood supply of the mandibular cortex: an experimental study in Gottingen minipigs with special reference to the condyle. J Craniomaxillofac Surg **30,** 41, 2002.
67. Kline, T.L., Zamir, M., and Ritman, E.L. Accuracy of microvascular measurements obtained from micro-CT images. Ann Biomed Eng **38,** 2851, 2010.
68. Rouwkema, J., de Boer, J., and Van Blitterswijk, C.A. Endothelial cells assemble into a 3-dimensional prevascular network in a bone tissue engineering construct. Tissue Eng **12,** 2685, 2006.
69. Kneser, U., Polykandriotis, E., Ohnolz, J., *et al.* Engineering of vascularized transplantable bone tissues: induction of axial vascularization in an osteoconductive matrix using an arteriovenous loop. Tissue Eng **12,** 1721, 2006.
70. Fedorovich, N.E., Haverslag, R.T., Dhert, W.J., and Alblas, J. The role of endothelial progenitor cells in prevascularized bone tissue engineering: development of heterogeneous constructs. Tissue Eng Part A **16,** 2355, 2010.
71. Huang, Y.C., Kaigler, D., Rice, K.G., Krebsbach, P.H., and Mooney, D.J. Combined angiogenic and osteogenic factor delivery enhances bone marrow stromal cell-driven bone regeneration. J Bone Miner Res **20,** 848, 2005.
72. Fang, T.D., Salim, A., Xia, W., *et al.* Angiogenesis is required for successful bone induction during distraction osteogenesis. J Bone Miner Res **20,** 1114, 2005.
73. Pacicca, D.M., Patel, N., Lee, C., *et al.* Expression of angiogenic factors during distraction osteogenesis. Bone **33,** 889, 2003.
74. Kleinheinz, J., Stratmann, U., Joos, U., and Wiesmann, H.P. VEGF-activated angiogenesis during bone regeneration. J Oral Maxillofac Surg **63,** 1310, 2005.
75. Simons, M., Alitalo, K., Annex, B.H., *et al.* State-of-the-art methods for evaluation of angiogenesis and tissue vascularization: a scientific statement from the American Heart Association. Cir Res **116,** e99, 2015.
76. Fei, J., Peyrin, F., Malaval, L., Vico, L., and Lafage-Proust, M.H. Imaging and quantitative assessment of long bone vascularization in the adult rat using microcomputed tomography. Anat Rec (Hoboken) **293,** 215, 2010.
77. Leong-Poi, H. Molecular imaging using contrast-enhanced ultrasound: evaluation of angiogenesis and cell therapy. Cardiovasc Res **84,** 190, 2009.
78. Lethaus, B., Poort, L., Yamauchi, K., Kloss-Brandstatter, A., Boeckmann, R., and Kessler, P. Qualitative bone CT as a tool to assess vascularization in irradiated bone: an animal study. Clin Oral Implants Res **24,** 746, 2013.
79. Bouxsein, M.L., Boyd, S.K., Christiansen, B.A., Guldberg, R.E., Jepsen, K.J., and Muller, R. Guidelines for assessment of bone microstructure in rodents using micro-computed tomography. J Bone Miner Res **25,** 1468, 2010.
80. Guldberg, R.E., Ballock, R.T., Boyan, B.D., *et al.* Analyzing bone, blood vessels, and biomaterials with microcomputed tomography. IEEE Eng Med Biol Mag **22,** 77, 2003.
81. Dai, J., and Rabie, A.B. VEGF: an essential mediator of both angiogenesis and endochondral ossification. J Dent Res **86,** 937, 2007.
82. Chung, A.S., and Ferrara, N. Developmental and pathological angiogenesis. Ann Rev Cell Dev Biol **27,** 563, 2011.
83. Glowacki, J. Angiogenesis in fracture repair. Clin Orthop Relat Res **355,** S82, 1998.

Address correspondence to:
Teja Guda, PhD
Department of Biomedical Engineering
University of Texas at San Antonio
One UTSA Circle, AET 1.356
San Antonio, TX 78249

E-mail: teja.guda@utsa.edu

Received: August 8, 2019
Accepted: October 28, 2019
Online Publication Date: December 13, 2019